Journal of Systemics, Cybernetics and Informatics (2022) 20(3), 24-30
https://doi.org/10.54808/JSCI.20.03.24

# Cell Behavior During Accelerated Passing through Micro-gap

**Shogo UEHARA**
Biomedical Engineering, Systems Design, Kogakuin University
Tokyo, 163-8677, Japan

**Shigehiro HASHIMOTO**
Biomedical Engineering, Department of Mechanical Engineering, Kogakuin University
at13351@g.kogakuin.jp Tokyo, 163-8677, Japan

**Sakyo SHIMADA**
Biomedical Engineering, Department of Mechanical Engineering, Kogakuin University
Tokyo, 163-8677, Japan

**Ayaka KURIHARA**
Biomedical Engineering, Department of Mechanical Engineering, Kogakuin University
Tokyo, 163-8677, Japan

## ABSTRACT[1]

A biological cell is flexible and must deform to pass through a narrow gap. Therefore, in capillaries and in liver and spleen sinusoids, vascular constrictions plays the role of a filter to sort healthy from damaged cells *in vivo*. In this study, deformation of a cell during accelerated passage through a microgap in a microflow channel was analyzed *in vitro*. A gap with the rectangular cross section (7 μm height, 0.8 mm width, and 0.1 mm length) was inserted at the middle of a microflow channel using photolithography. Myoblasts (C2C12: mouse myoblast cells) were used in the test. The flow rate of the medium fluid, in which cells were suspended, was controlled by the pressure head between the inlet and outlet. The deformation of smaller cells passing through the microgap with an accelerated velocity was observed with an inverted phase-contrast microscope. The results show that each elongated smalller (diameter < 15 μm) cell tends to tilt parallel to the flow direction during its transit through the gap.

**Keywords**: Biomedical Engineering, Myoblast, Movement, Deformation, Photolithography and Microgap.

## 1. INTRODUCTION

The deformation of the biological cell relates to the biological function. Several types of the cells can pass through a narrow slit *in vivo*. A red blood, for example, cell has a high flexibility, hence can pass through the micro capillary in the blood circulation system *in vivo*. The red blood cell passes through the capillary, of which the dimension is smaller than the diameter of itself. It deforms from the biconcave disk shape to the parachute like shape when it is passing through the capillary. The membrane elasticity [1] and fatigue [2] were evaluated in the previous studies. In the shear field, the red blood cell rotates and deforms into the ellipsoidal shape. The deformability of a red blood cell changes with aging. The aging effect on deformability [3] and the sublethal damage [4] were also detected in the shear flow in the previous studies *in vitro*. After the circulation through the blood circulation system for days, the red blood cell is trapped in the micro-circulation systems.

Several systems sort cells according to the deformability *in vivo*. One of the systems, which trap red blood cells, is a spleen. The spleen has special morphology at the blood flow path to sort damaged red blood cells [5]. A slit is one of the systems, which sorts biological cells *in vivo*. The sorting at the slit depends on the deformability of each cell. Some cells can pass through a very narrow gap.

A photolithography technique enables manufacturing micro grooves [6-10] or micro-structures [11] in the flow-channel for cell tests *in vitro*. Several micro-fabrication processes have been designed to simulate the morphology of the micro-circulation [12]. The technique also has been applied to handle cancer cells in diagnostics *in vitro* [13, 14]. The photolithography technique can be applied to make a microgap. The gap between micro cylinders, for example, was made to sort cells in the previous study [15].

The deformation of the depth direction between cylinders, however, cannot be observed by the

[1] The authors are grateful to Prof. Richard L. Magin for assistance in the English Editing of this article.

conventional optical microscope. To observe the deformed cell in the direction perpendicular to the walls of the gap, another type of the gap was designed with the combination of microridges in the previous study [16-21]. In the present study, deformation of a cell during passage through a microgap in a micro flow-channel has been analyzed *in vitro*.

## 2. METHODS

### Micro Gap

A microgap was designed between a transparent polydimethylsiloxane (PDMS) plate and a borosilicate glass (Tempax) plate. The upper plate of PDMS has a rectangular ridge: 0.05 mm high, 0.10 mm wide, and 2 mm long. The lower plate of glass has a rectangular groove (7 μm deep, 2 mm wide, and 20 mm long), which has a narrow part (0.8 mm wide). These plates make contact to keep a gap (0.8 mm wide, 0.1 mm long and 7 μm high) between them.

### Flow Channel

The upper plate of PDMS was rinsed with IPA, and with the ultrapure water. The plate was dried by a spin-dryer. The surface of the PDMS plate was hydrophilized by the oxygen (30 $cm^3$/min, 0.1 Pa) plasma ashing for thirty seconds at 50 W by the reactive ion etching system (FA-1). The plate was rinsed with APTES (Aminopropyl-triethoxysilane) for five minutes and dipped in the ultrapure water. The plate was dried in an oven at 338 K for three minutes. The upper plate of PDMS was adhered on the lower plate of SU8-10 to make the gap between the plates. The combined plates were baked on a heated plate at 338 K for five minutes.

### Flow Test

C2C12 (passage < 10, mouse myoblast cell line originated with cross-striated muscle of C3H mouse) was used in the test. Cells were cultured in advance with the D-MEM (Dulbecco's Modified Eagle's Medium) containing 10% FBS and 1% of Antibiotic-Antimycotic (penicillin, streptomycin and amphotericin B, Life Technologies) in the incubator for one week. The inner surface of the flow channel was hydrophilized by the oxygen (30 $cm^3$/min, 0.1 Pa) plasma ashing for one minute at 100 W by the reactive ion etching system (FA-1), and prefilled with the bovine serum albumin solution for thirty minutes at 310 K.

Just before the flow test, the cells were exfoliated from the plate of the culture dish with trypsin and suspended in the D-MEM (Dulbecco's Modified Eagle's Medium). The suspension of cells (4000 cells/$cm^3$, 0.06 $cm^3$) was poured into the inlet of the flow channel. The flow occurs by the pressure difference between the fluid levels of the inlet and the outlet (Fig. 1). The small reservoir (the depth of 3 mm and the diameter of 5 mm) at the inlet keeps the pressure head. The behavior of cells near the gap was observed with an inverted phase-contrast microscope (IX71, Olympus Co., Ltd., Tokyo) at 298 K. The microscopic movie images of thirty frames per second at the shutter speed of 1/2000 s were recorded by the camera (DSC-RX100M4, Sony Corporation, Tokyo, Japan).

### Image of Cell

At the two-dimensional image, the contour of each cell was traced, and analyzed by "ImageJ". The projected two-dimensional area ($S$) was calculated. The contour was approximated to the ellipse (Fig. 2). On the ellipse, both the length of the major axis ($a$) and the length of the minor axis ($b$) were measured (Fig. 3). The ratio of axes is calculated as the shape index ($P$) by Eq. (1).

$$P = 1 - b / a \tag{1}$$

At the circle, $P = 0$. As the ellipse lengthens ($a > b$), $P$ approaches to 1.

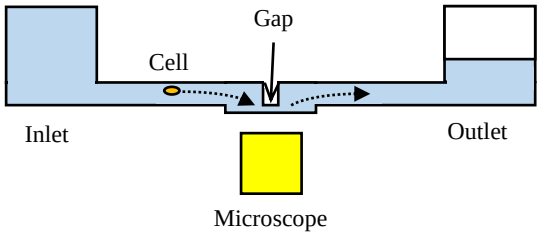


**Fig. 1:** Flow was generated by pressure head at inlet, and behavior of cell passing through gap was observed by microscope.

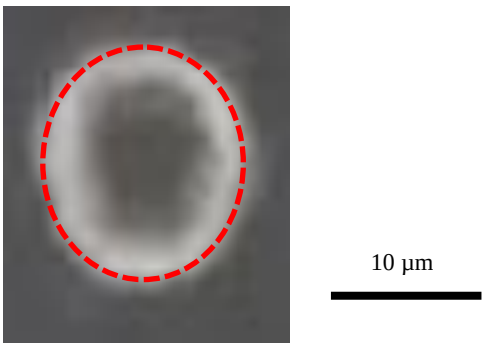


**Fig. 2:** Contour of two-dimensional projected image of cell was approximated to ellipse (broken line).

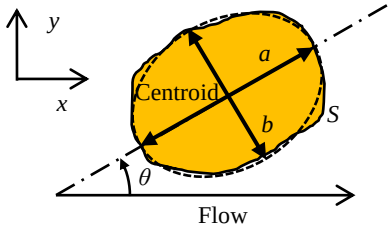


**Fig. 3:** Contour of two-dimensional projected image ($S$) of cell was approximated to ellipse (broken line): major axis ($a$), minor axis ($b$) and angle ($\theta$) were measured.

The centroid was used to track each flowing cell. The coordinates were defined as follows: the $x$ axis is parallel to the mainstream direction, and the $y$ axis is perpendicular to the mainstream direction (Fig. 3). The acute angle $\theta$ (– 90 degrees < $\theta$ < 90 degrees) between the major axis of the ellipse and the mainstream direction of the medium flow was measured (Fig. 3). When the major axis of the cell is parallel to the flow direction, $\theta$ is zero.

## 3. RESULTS

Several cells passed through the gap in a few seconds (Fig. 4). Data of cells accelerated in the microgap were selected in the following figures.

Figs. 5-8 show tracings of cell behavior through the micro gap. The data related to position $x$ along the flow channel were illustrated. The microgap is located from 980 μm to 1080 μm for $x$. In Figs. 5-8, circle markers show data in the micro-gap.

Fig. 5 shows the velocity ($v$). The velocity of the cell is three times higher in the gap than outside of the gap. The ratio of the cross section of the gap to the channel is as follows: 7 μm × 0.8 mm / 50 μm × 0.8 mm. The continuity equation shows a ratio of 7 times the velocity between the gap and the channel. The velocity of the cell was slower than that of the fluid in the gap.

Fig. 6 shows the projected two-dimensional area ($S$) of the cell. The area increases (30%) in the gap and decreases as it passes through the gap. The projected two-dimensional region ($S$) of the cell takes some time after passing through the microgap to return to the value before the microgap.

The tracing of the shape index $P$ is illustrated in Fig. 7. The value fluctuates between 0 and 0.2. The fluctuation decreases in the microgap. Immediately after passing through the microgap, the shape index increases to 0.3.

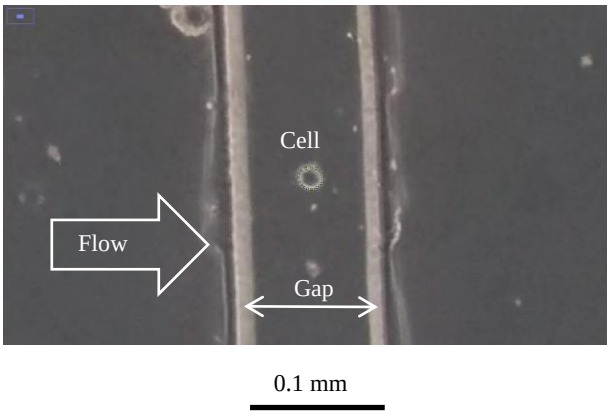


**Fig. 4:** Cell passing through microgap.

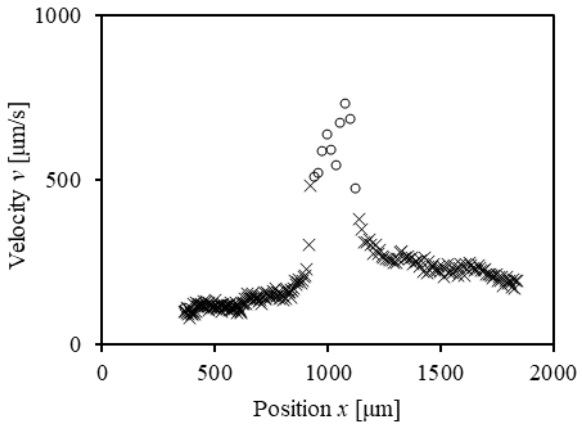


**Fig. 5:** Velocity $v$ tracings of a cell passing through gap (980 μm < $x$ < 1080 μm): circle, data in gap: cross, data out of gap.

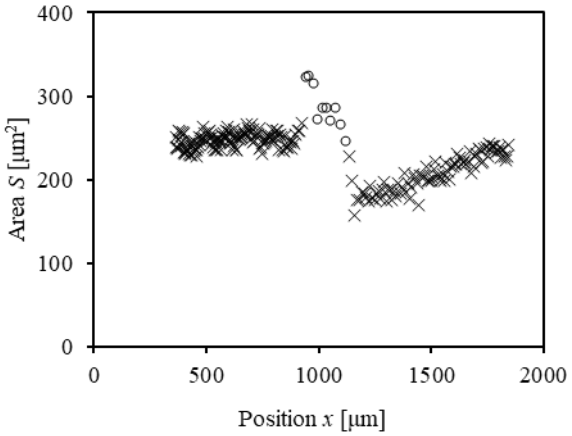


**Fig. 6:** Area $S$ tracings of a cell passing through gap (980 μm < $x$ < 1080 μm): circle, data in gap: cross, data out of gap.

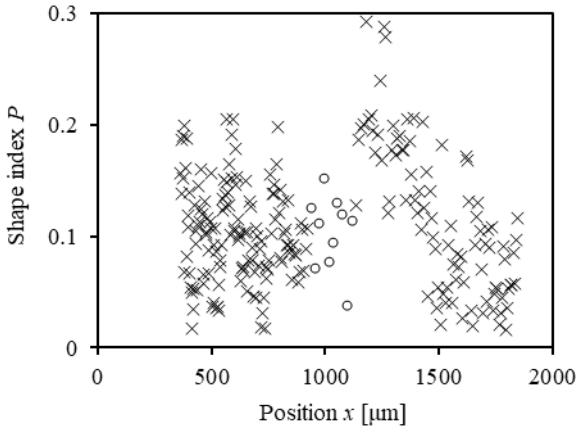


**Fig. 7:** Shape index $P$ tracings of a cell passing through gap (980 μm < $x$ < 1080 μm): circle, data in gap: cross, data out of gap.

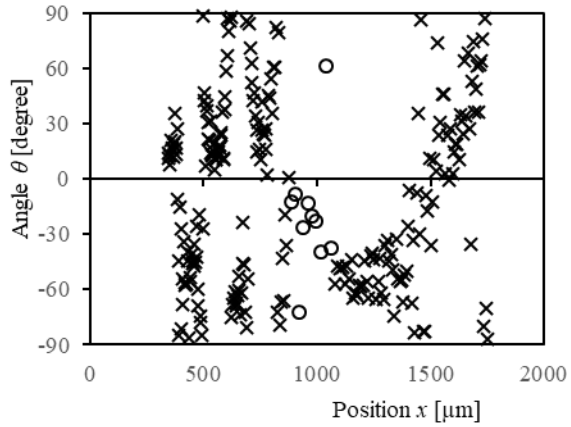


**Fig. 8:** Angle $\theta$ tracings of cell passing through gap (980 μm < $x$ < 1080 μm): circle, data in gap: cross, data out of gap.

Fig. 8 shows the tracings of the angle $\theta$ between the major axis of the cell and the mainstream direction of the medium fluid. The angle tends to approach 0 degrees in the microgap. The angle fluctuates after passing through the microgap.

Fig. 9 shows the relationship between the shape index $P$ and the projected two-dimensional area ($S$) of the cell: before the micro-gap (Fig. 9a), and in the microgap (Fig. 9b). Fig. 9 shows no clear relationships between two parameters.

Fig. 10 shows the relationship between the angle $\theta$ and the shape index $P$ of the cell: before the microgap (Fig. 10a), and in the microgap (Fig. 10b). The angle tends to decrease as the shape index increases before the microgap. The tendency is maintained in the microgap. The tendency becomes weak in the microgap.

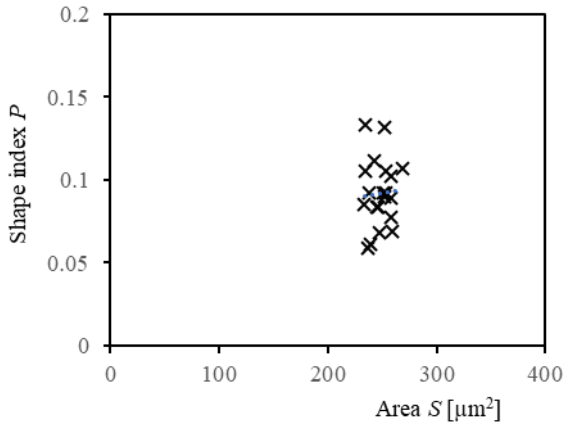


**Fig. 9a:** Shape index $P$ vs. area of a cell $S$ before gap: $P$= 0.0001 $S$ + 0.067, $r$ = 0.05.

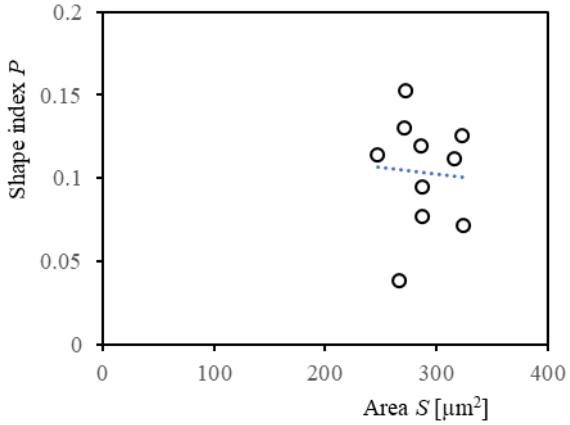


**Fig. 9b:** Shape index $P$ vs. area $S$ of a cell in gap: $P = -7 \times 10^{-5} S + 0.12$, $r$ = 0.06.

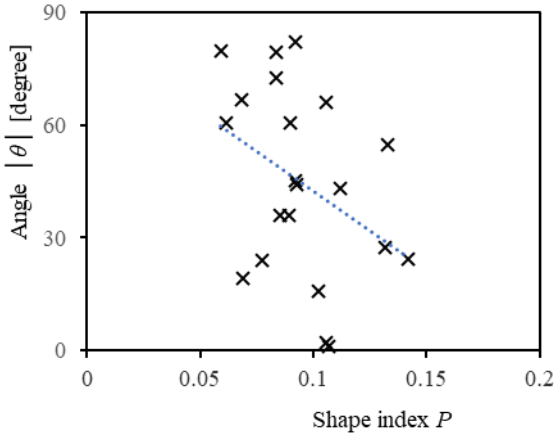


**Fig. 10a:** Angle $|\theta|$ vs. shape index $P$ before gap: $|\theta| = -4.2 \times 10^{2} P + 84$, $r$ = 0.38.

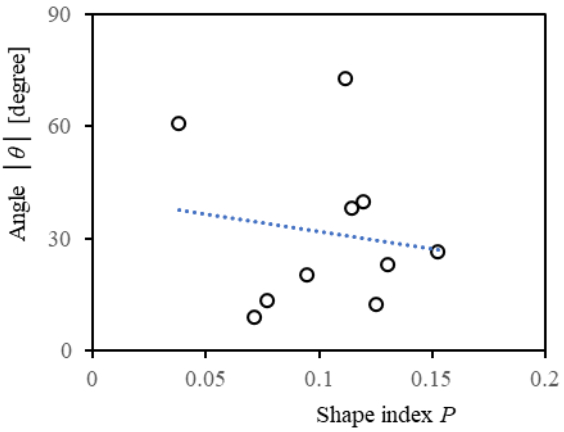


**Fig. 10b:** Angle $|\theta|$ vs. shape index $P$ in gap: $|\theta| = -94\,P + 41$, $r = 0.15$.

## 4. DISCUSSION

For the reason of the limitation of the present micromachining technique with the photolithography process, the edge of the ridge is not sharp. The edge has a certain width. The biological system has the sharper edge, so that a cell passes easier through the slit with the shorter travel distance *in vivo* [5]. The cell has to struggle to pass through the gap in the present experimental device with the longer travel distance. The relationship between cell deformation and the flow of intracellular contents was investigated in previous studies [22]. The relationship between wall roughness and the speed of red blood cells passing through microchannels was studied [23].

The dimension of the gap was estimated by observing the passing velocity of porcine red blood cells in the present study. The ratio of the cross-sectional area between the flow channel (0.05 mm × 0.8 mm) and the gap (0.007 mm × 0.8 mm) was 7. Using continuity of the fluid, the mean flow velocity of the medium in the gap is 7 times faster than that before the gap. In the cell selected in this study, the velocity ratio inside the micro-gap to outside the micro-gap was close to 7. (Fig. 5). The area $S$ of the circle is calculated by the radius $R$ using Eq. (2).

$$S = \pi R^2 \tag{2}$$

When $S$ is 250 μm$^2$, $R$ is 8.9 μm. The equivalent radius of the sphere of the selected cells (Fig. 6) is close to the height of the micro-gap.

In the previous study [15], the flow rate was controlled by the syringe pump. In that case, the flow rate varied because of several factors: the compliance of the wall of the flow path, and clogging of the flow path. The flow rate is controlled by the pressure difference between inlet and outlet of the flow channel in the present study, which has advantage to keep the inner pressure of the flow channel for the morphological stability of the flow channel. The velocity of a cell also depends on the interaction between the cell and the surface of the micro-gap. To keep the inner surface of the channel stable, bovine serum albumin was pre-coated on the surface of the flow path by prefilling the bovine serum albumin solution in the channel in this study.

Biological cells are sorted according to the shape, and deformability *in vivo*. Several cells pass through the micro-slit. Some cells or fragments, which pass through the slit, are decomposed. Some cells, which cannot pass through the narrow channel, are, on the other hand, captured at the channel.

The deformability of the biological single cell depends on several factors. The deformability has been analyzed in several studies: using microfluidics [24-26], measuring local viscoelasticity [27], using atomic force microscopy [28 29], and using cell mechanics model [30]. The methodology can also be applied to the soring technology on cells [31-33]. The deformation in the gap was evaluated with the ratio of the projected area of the plan view of the disk-like shape during passing through the gap in the previous study [34]. The deformation in the perpendicular view can be observed at another type of the gap: between micro cylindrical pillars [15].

The most of biological cells keep the spherical shape when they are flowing in the medium. In the previous experiment, every myoblast cell was deformed when the cell was passing through the microgap with the height of 7 μm [34]. The nucleus in the cell has low deformability [35, 36].

The increase in the two-dimensional projected area in the gap may depend on the deformation of the cell (Fig. 6). The fact that the velocity increases in the gap as well as the surrounding fluid (Fig. 5) is considered to correspond to the weak interaction between the cells and the gap wall surface. The cell size taken up in Fig. 5 may be the limit of passing through the microgap without intermittent stops. This corresponds to the smaller variation in gap flattening. The cell size can be applied to distinguish by interaction with the wall surface. The recovery tendency of the two-dimensional projected area after passing through the gap (Fig. 6) can also be applied to the observation of cell deformation behavior similar to erythrocytes [37].

The fluctuation of the shape index before the microgap may be related to the change in the two-dimensional projection plane direction with the rotation of the cell (Fig. 7). Other than the sphere, the two-dimensional projected area depends on the direction. The microgap limits cell rotation and can reduce variations in two-dimensional projected area. The increase in flattening

immediately after passing through the gap is considered to reflect the partial deformation of the cells. The change in the direction of the major axis of the cell before the gap (Fig. 8) may reflect the effect of cell rotation. The microgap limits cell rotation and can reduce the fluctuation in the major axis direction (Fig. 8). Immediately after passing through the gap, the hysteresis effect of deformation within the gap can reduce the fluctuation in the major axis direction. The behavior of the cell may return to that before the gap after the deformation has recovered downstream.

No correlation was found between the shape index and two-dimensional projected area (Fig. 9). Similarly, no correlation was found between the shape index and the two-dimensional projected area when larger (diameter > 20 μm) cells were trapped and moved in the gap in the previous study [34]. As the shape index decreases (the two-dimensional projection plane approaches a circle), the major axis direction tends to fluctuate. The major axis tilts to the direction perpendicular to the flow (Fig. 10a). When a cell can rotate freely, the major axis tends to tilt in the flow direction (the absolute value of $\theta$ decreases in Fig. 10a). The major axis of the cell tends to tilt in the direction of flow under restriction of rotation in the micro-gap (the absolute value of $\theta$ in Fig. 10b tends to be less than 45 degrees). As the deformation progresses, the major axis tends to tilt in the direction of the flow. When a larger cell moves intermittently in the gap with deformation, the major axis of the cell tends to tilt perpendicular to the flow [34]. The designed microgap can be used to analyze the mechanism of deformation of the single biological cell to pass through the gap.

## 5. CONCLUSIONS

Deformation of cells during accelerated passing through a micro-gap in a micro flow channel was analyzed *in vitro*. The experimental results show that the elongated myoblasts tend to tilt parallel to the flow direction during accelerated passing through the gap.

## ACKNOWLEDGMENT

The authors thank Dr. Yusuke Takahashi, Mr. Yuki Takiguchi and Mr. Shoki Toyota for their help of the experiment.

## REFERENCES

[1] J. Sleep, D. Wilson, R. Simmons and W. Gratzer, "Elasticity of the Red Cell Membrane and Its Relation to Hemolytic Disorders: An Optical Tweezers Study", **Biophysical Journal**, Vol. 77, No. 6, 1999, pp. 3085-3095.

[2] S. Sakuma, K. Kuroda, C.H.D. Tsai, W. Fukui, F. Arai and M. Kaneko, "Red Blood Cell Fatigue Evaluation Based on the Close-encountering Point between Extensibility and Recoverability", **Lab on a Chip**, Vol. 14, 2014, pp. 1135-1141.

[3] S. Hashimoto, H. Otani, H. Imamura, et al., "Effect of Aging on Deformability of Erythrocytes in Shear Flow", **Journal of Systemics Cybernetics and Informatics**, Vol. 3, No. 1, 2005, pp. 90-93.

[4] S. Hashimoto, "Detect of Sublethal Damage with Cyclic Deformation of Erythrocyte in Shear Flow", **Journal of Systemics Cybernetics and Informatics**, Vol. 12, No. 3, 2014, pp. 41-46.

[5] L.T. Chen and L. Weiss, "The Role of the Sinus Wall in the Passage of Erythrocytes through the Spleen", **Blood**, Vol. 41, No. 4, 1973, pp. 529-537.

[6] Y. Takahashi, S. Hashimoto, H. Hino, A. Mizoi and N. Noguchi, "Micro Groove for Trapping of Flowing Cell", **Journal of Systemics, Cybernetics and Informatics**, Vol. 13, No. 3, 2015, pp. 1-8.

[7] S. Hashimoto, Y. Takahashi, H. Hino, R. Nomoto and T. Yasuda, "Micro Hole for Trapping Flowing Cell", **Proc. 18th World Multi-Conference on Systemics Cybernetics and Informatics**, Vol. 2, 2014, pp. 114-119.

[8] S. Hashimoto and W. Sekine, "How Does Cell Change Flow Direction in Micro Groove?", **Proc. 25th World Multi-Conference on Systemics Cybernetics and Informatics**, Vol. 3, 2021, pp. 37-42.

[9] S. Hashimoto, T. Matsumoto, S. Uehara and Y. Endo "Bumping Movement of Cell Flowing over Oblique Micro-groove: Comparison with Movement Outside Groove", **Proc. 13th International Multi-Conference on Complexity Informatics and Cybernetics**, Vol. 2, 2022, pp. 23-28.

[10] S. Hashimoto, S. Uehara and H. Yonezawa, "Behavior of Cell Flowing Over Oblique Micro Rectangular Groove", **Proc. ASME International Mechanical Engineering Congress & Exposition (IMECE2021)**, 2021, pp. 1-6.

[11] S. Hou, H. Zhao, L. Zhao, Q. Shen, K.S. Wei, D.Y. Suh, A. Nakao, M.A. Garcia, M. Song, T. Lee, B. Xiong, S.C. Luo, H.R. Tseng and H.H. Yu, "Capture and Stimulated Release of Circulating Tumor Cells on Polymer-Grafted Silicon Nanostructures", **Advanced Materials**, Vol. 25, No. 11, 2013, pp. 1547-1551.

[12] L.M. Lee and A.P. Liu, "A Microfluidic Pipette Array for Mechanophenotyping of Cancer Cells and Mechanical Gating of Mechanosensitive Channels", **Lab on a Chip**, Vol. 15, 2015, pp. 264-273.

[13] J.E. Shim, J. Bu, M.K. Lee, Y.H. Cho, T.H. Kim, J.U. Bu and S.W. Han, "Viable and High-throughput Isolation of Heterogeneous Circulating Tumor Cells Using Tapered-slit Filters", **Sensors and Actuators B: Chemical**, Vol. 321, 2020, 128369, pp. 1-8.

[14] M. Hakim, F. Khorasheh, I. Alemzadeh and M. Vossoughi, "A New Insight to Deformability Correlation of Circulating Tumor Cells with

Metastatic Behavior by Application of a New Deformability-based Microfluidic Chip", **Analytica Chimica Acta**, Vol. 1186, 2021, 339115, pp. 1-8.

[15] Y. Takahashi, S. Hashimoto, H. Hino and T. Azuma, "Design of Slit between Micro Cylindrical Pillars for Cell Sorting", **Proc. 20th World Multi-Conference on Systemics Cybernetics and Informatics**, Vol. 2, 2016, pp. 165-170.

[16] S. Hashimoto, A. Mizoi, H. Hino, K. Noda, K. Kitagawa and T. Yasuda, "Behavior of Cell Passing through Micro Slit", **Proc. 18th World Multi-Conference on Systemics Cybernetics and Informatics**, Vol. 2, 2014, pp. 126-131.

[17] A. Mizoi, Y. Takahashi, H. Hino, S. Hashimoto and T. Yasuda, "Deformation of Cell Passing through Micro Slit", **Proc. 19th World Multi-Conference on Systemics Cybernetics and Informatics**, Vol. 2, 2015, pp. 270-275.

[18] Y. Takahashi, S. Hashimoto, A. Mizoi and H. Hino, "Deformation of Cell Passing through Micro Slit between Micro Ridges Fabricated by Photolithography Technique", **Journal of Systemics, Cybernetics and Informatics**, Vol. 15, No. 3, 2017, pp. 1-9.

[19] S. Uehara and S. Hashimoto, "How Does Cell Deform during Movement in Micro Gap?", **Proc. 25th World Multi-Conference on Systemics Cybernetics and Informatics**, Vol. 3, 2021, pp. 31-36.

[20] S. Hashimoto, K. Yoshinaka and H. Yonezawa, "Behavior of Cell Passing Through Micro Slit Between Micro Machined Plates", **Proc. ASME Fluids Engineering Division Summer Meeting (FEDSM2021)**, 2021, pp. 1-6.

[21] S. Hashimoto, S. Shimada and S. Uehara, "Direction of Cell Deformation During Microgap Passage", **Proc. 13th International Multi-Conference on Complexity Informatics and Cybernetics**, Vol. 2, 2022, pp. 17-22.

[22] E.F. Koslover, C.K. Chan and J.A. Theriot, "Cytoplasmic Flow and Mixing Due to Deformation of Motile Cells", **Biophysical Journal**, Vol. 113, No. 9, 2017, pp. 2077-2087, 2017.

[23] N.A. Besedina, E.A. Skverchinskaya, A.S. Ivanov, K.P. Kotlyar, I.A. Morozov, N.A. Filatov, I.V. Mindukshev and A.S. Bukatin, "Microfluidic Characterization of Red Blood Cells Microcirculation under Oxidative Stress", **Cells**, Vol. 10, No. 12, 2021, p. 3552.

[24] B. Deng, H. Wang, Z. Tan and Y. Quan, "Microfluidic Cell Trapping for Single-Cell Analysis", **Micromachines**, Vol. 10, No. 6, 409, 2019, pp. 1-10.

[25] S.J. Hymel, H. Lan and D.B. Khismatullin, "Elongation Index as a Sensitive Measure of Cell Deformation in High-Throughput Microfluidic Systems", **Biophsycal Journal**, Vol. 119, No. 3, 2020, pp. 493-501.

[26] F.J. Armistead, J.G. De Pablo, H. Gadêlha, S.A. Peyman and S.D. Evans, "Cells Under Stress: An Inertial-shear Microfluidic Determination of Cell Behavior", **Biophsycal Journal**, Vol. 116, No. 6, 2019, pp. 1127-1135.

[27] A.R. Bausch, W. Moeller and E. Sackmann, "Measurement of Local Viscoelasticity and Forces in Living Cells by Magnetic Tweezers", **Biophysical Journal**, Vol. 76, No. 1, 1999, pp. 573-579.

[28] E. A-Hassan, W.F. Heinz, M.D. Antonik, N.P. D'Costa, S. Nageswaran, C.-A. Schoenenberger and J.H. Hoh, "Relative Microelastic Mapping of Living Cells by Atomic Force Microscopy", **Biophysical Journal**, Vol. 74, No. 3, 1998, pp. 1564-1578.

[29] S.E Cross, Y.-S. Jin, J. Tondre, R. Wong, J.Y. Rao and J.K. Gimzewski, "AFM-based Analysis of Human Metastatic Cancer Cells", **Nanotechnology**, Vol. 19, No. 38, 2008, 384003, pp. 1-8.

[30] G. Bao and S. Suresh, "Cell and Molecular Mechanics of Biological Materials", **Nature Materials**, Vol. 2, No. 11, 2003, pp. 715-725.

[31] B. Lincoln, H.M. Erickson, S. Schinkinger, F. Wottawah, D. Mitchell, S. Ulvick, C. Bilby and J. Guck, "Deformability-Based Flow Cytometry", **Cytometry**, Part A: the Journal of the International Society for Analytical Cytology, Vol. 59, No. 2, 2004, pp. 203-209.

[32] Y. Takahashi, S. Hashimoto and M. Watanabe, "Dielectrophoretic Movement of Cell around Surface Electrodes in Flow Channel", **Journal of Systemics Cybernetics and Informatics**, Vol. 16, No. 3, 2018, pp. 81-87.

[33] S. Hashimoto and K. Yoshinaka, "Movement of Myoblast Flowing Through Electric Field Perpendicular to Flow Channel", **Proc. ASME Fluids Engineering Division Summer Meeting (FEDSM2021)**, 2021, pp. 1-10.

[34] S. Hashimoto, "Cell Behavior in Flow Passing through Micro Machined Gap", **ASME Journal of Engineering and Science in Medical Diagnostics and Therapy** (JESMDT-22-1006), Vol. 5, No. 4, 2022, pp. 1-6.

[35] E. Antmen, U. Demirci and V. Hasirci, "Micropatterned Surfaces Expose the Coupling between Actin Cytoskeleton-Lamin/Nesprin and Nuclear Deformability of Breast Cancer Cells with Different Malignancies", **Advanced Biology**, Vol. 5, No. 2000048, 2021, pp. 1-14.

[36] I.D. Estabrook, H.R. Thiam, M. Piel and R.J. Hawkins, "Calculation of the Force Field Required for Nucleus Deformation during Cell Migration through Constrictions", **PLoS Computational Biology**, Vol. 17, No. 5, 2021, e1008592.

[37] C. Bernecker, M.A.R.B.F. Lima, C.D. Ciubotaru, P. Schlenke, I. Dorn and D. Cojoc, "Biomechanics of Ex Vivo-Generated Red Blood Cells Investigated by Optical Tweezers and Digital Holographic Microscopy", **Cells**, Vol. 10, No. 552, 2021, pp. 1-18.